Electronic transport by small polarons in $La_{0.5}Sr_{0.5}MnO_3$

E. Quenneville, M. Meunier,[a] and A. Yelon
Groupe de Recherche en Physique et Technologie des Couches Minces (GCM) and Department of Engineering Physics, École Polytechnique de Montréal, C.P. 6079, succ. Centre-Ville, Montréal (Québec), Canada, H3C 3A7

F. Morin
Institut de Recherche d'Hydro-Québec, Chimie et Environment, 1800 Montée Lionel Boulet, Varennes (Québec), Canada, J3X 1S1

(Received 3 November 2000; accepted for publication 18 May 2001)

Electrical conductivity measurements on $La_{0.5}Sr_{0.5}MnO_3$ (LSM5) thin films as a function of temperature are presented. These are used to demonstrate that the electronic transport in LSM5 is well described by the Emin–Holstein adiabatic small polaron model. Measurements have also been performed on bulk samples. Even if the conductivity behaves somewhat differently in the latter case, the same polaronic model still applies. The polaron densities extracted from conductivity measurements are very similar, ranging from 7 to $8\times10^{21}\,cm^{-3}$ for thin films and are $9.1\times10^{21}\,cm^{-3}$ for bulk samples. These results agree quite well with the nominal polaron density for LSM5, $8.4\times10^{21}\,cm^{-3}$. We have also derived important quantities for transport in LSM5. For thin films, we obtained hopping energies, W_H, ranging between 73 and 99 meV and almost constant, at 34 meV, for bulk samples. By fitting conductivity measurements from 50 to 1123 K, we also find the zero point interaction constant, γ_0, to be 0.35 in thin films. These conductivity results are compared with the literature. © *2001 American Institute of Physics.* [DOI: 10.1063/1.1385356]

I. INTRODUCTION

Lanthanum manganite doped with either calcium or strontium has received much attention in recent years, due to the large magnetoresistance observed in many of these perovskites.[1–3] Most studies have concentrated on thin film samples at low temperatures. $La_{1-x}Sr_xMnO_3$ has proved to be an efficient cathode material for solid oxide fuel cells.[4,5] In this case, most of the present knowledge relates to low degrees of strontium substitution with $x\leqslant0.3$. Reequilibration in these cation-defective materials with the surrounding atmosphere often proceeds slowly even at rather high temperatures. Hence, the use of thin films is useful for the study of physical properties in conditions close enough to chemical equilibrium. $La_{0.5}Sr_{0.5}MnO_3$ (LSM5) is an appropriate composition for such studies. Pulsed laser deposition followed by annealing transfers composition from target to film, producing LSM5 films with the desired chemical composition and film morphology.[6,7]

There have been few reports on LSM5 electrical properties in bulk samples[8–11] and in thin films.[12,13] The electronic transport in bulk samples and in polycrystalline thin films are investigated here. To obtain the most information from the conductivity measurements on LSM5, it is important to determine the main transport mechanism responsible for the high electrical conductivity in this material. For similar compounds, it has been shown from various measurements, (e.g., optical,[14–16] thermoelectric power,[17,18] Hall effect[17]), that the electronic conductivity is well described by a polaronic mechanism. It is generally accepted that the electronic transport in bulk LSM5 is correctly described by the small polaron hopping model.[8,10–12,19] However, in order to extract significant physical parameters from experimental data, discrimination between the adiabatic and the nonadiabatic cases should be made. Moreover, if the charge carrier mobility is high enough, correlation between hops may considerably reduces the hopping energy.[20] These points from the literature need to be further clarified for LSM5.

The combination of total conductivity and thermoelectric power measurements has been used successfully in the literature for the study of electrical transport in low mobility materials.[17,18,21] Thermoelectric power measurements are interpreted far more readily than Hall effect measurements,[21,22] particularly for high resistance samples.[23] It can be shown that the slope of the thermoelectric power versus the reciprocal of temperature is identical to the activation energy for conductivity, provided the carrier mobility is unactivated. If, however, transport proceeds by a hopping mechanism, then the difference in the earlier energies would be an approximate measurement of the hopping activation energy.[24] In this work, a combination of total conductivity at high and at low temperatures is used for the study of electronic transport in LSM5. Because the basic mechanisms involved are very different in these two temperature ranges, it will be shown that all parameters needed in the description of the thermal behavior of the conductivity can be extracted without using thermoelectric power measurements.

II. EXPERIMENT

In the present work, pulsed laser deposition was used to prepare 400-nm-thick LSM5 thin films on the *R*-plane of sapphire substrates. The experimental setup is described

[a]Author to whom correspondence should be addressed; electronic mail: meunier@phys.polymtl.ca

TABLE I. Pulsed laser deposition parameters.

Laser wavelength	248 nm
Repetition rate	30 Hz
Spot size	2 mm^2
Energy density	0.75 J/cm^2
Target-substrate distance	5.5 cm
Substrate	Sapphire (*R* plane)
Substrate temperature	25 °C
Deposition rate	~10 nm/min

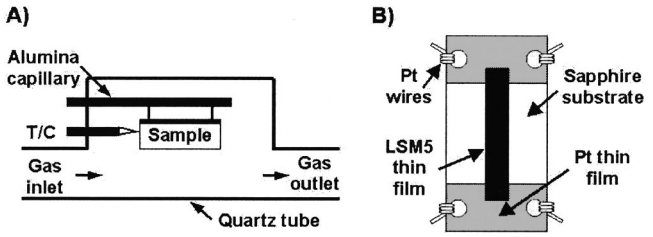

FIG. 1. (a) Schematic of the four-wire experimental setup for high temperature conductivity measurements. (b) Sketch showing the 400 nm×3 ×14 mm LSM5 thin film deposited onto a sapphire substrate between two platinum films 1 cm apart. The platinum wires are held in mechanical contact with the platinum films through holes drilled into the substrate.

elsewhere.[25] Films prepared under the conditions listed in Table I are amorphous. As reported in more detail elsewhere,[7] the resulting LSM5 films were analyzed by x-ray photoelectron spectroscopy, energy dispersive x-ray spectrometry, and Rutherford backscattering spectrometry (RBS) for their chemical composition. No departure from the nominal LSM5 composition was observed with these techniques. RBS measurements further showed that the films remained of uniform composition throughout their thickness. Film morphologies were observed by means of scanning electron microscopy and atomic force microscopy. The amorphous films were dense and pinhole free. The annealed films were polycrystalline and exhibited the expected perovskite structure as confirmed by x-ray diffraction (XRD). Some physical defects were observed in films annealed well above 1123 K probably due to stresses generated by the differential thermal expansion coefficient between the film and the substrate.[6]

LSM5 pellets for bulk conductivity measurements were fabricated from two different powders: one from an in-house (IREQ) synthesis with a modified glycine-nitrate process,[26] the other provided by Praxair. The pellets were prepared by cold isostatic pressing at about 300 MPa and brought to almost full density by firing for 4 h at 1400 °C in pure oxygen. As measured by an immersion method, the resulting pellets had densities respectively equal to 6.16 g/cm^3 for the starting Praxair powder and 6.22 g/cm^3 for the IREQ pellets. To promote grain growth, a further anneal was performed at 1550 °C for 4 h on some IREQ pellets, resulting in a density of 6.18 g/cm^3.

Most conductivity measurements were performed in air using a temperature ramp from room temperature for thin film samples. Intermediate plateaus for certain experiments ensured that the readings were fully stabilized at any temperature. To circumvent any electrical contact instability due to differential thermal expansion between materials, the four-wire setup shown in Figs. 1(a) and 1(b) was applied to thin film samples. The samples were held by an alumina capillary in a quartz tube at the center of a furnace. A type *R* thermocouple was placed in the vicinity of the sample and the gas supply was manifolded through the tube, the overall pressure being maintained at 1 atm. The 400 nm×3×14 mm LSM5 thin films were deposited onto a sapphire substrate between two platinum films separated by 1 cm. Four platinum wires were brought into mechanical contact with the Pt films by holes drilled throughout the substrate. A pair of wires injected a pulsed current through the LSM5 film and the corresponding potential drop recorded with a second pair. The resistance of the platinum layer and that of its interface with the LSM5 film then add to that of the LSM5 film proper. Since the latter is much larger, the two other contributions become negligibly small. Such is not the case for bulk samples and true four-point measurements were applied to these. Conductivity measurements on thin films configured as in Fig. 1(b) were also performed at low temperatures by means of a cold finger cryostat, Cryogenics Model 21. This cryostat permitted the measurements to be extended to the temperature range from 300 to 12 K.

The ionic contribution to the total conductivity of LSM5 is known to be several orders of magnitude lower than the electronic contribution. This is due to the high electron mobility and the lack of departure from stoichiometry from any of the sublattices within the temperature and the oxygen partial pressure ranges studied.[27] Thus, the total conductivity is assumed to be purely electronic in what follows.

III. RESULTS

Thin films prepared using the parameters of Table I are amorphous and need to be further annealed to become crystalline. Because amorphous LSM5 is an insulator and crystalline LSM5 a good electrical conductor, the recrystallization process is easily monitored using conductivity measurements. Figure 2 shows the conductivity, σ, as a function of temperature, *T*, for three successive annealing cycles in air at 1123, 1138, and 1158 K, respectively. For clarity, only results obtained during the decreasing part of the cycles are shown. The insert shows conductivity measurements for the first anneal at 1123 K on the initially amorphous thin film. Before 658 K, the resistance of the sample was too high to be measurable by the setup. The sudden increase in conductivity at around 870 K upon the first cycle is attributed to the phase transition from an amorphous state to the expected perovskite structure as also confirmed by XRD.[7] The conductivity further increases as temperature is raised to 1123 K. Partial reoxidation of the LSM5 films is also observed during this stage.[7] During the plateau at this latter temperature, the conductivity stabilizes after about an hour. Further cycling the sample up to this upper temperature leads to perfectly reproducible results (within 2%). The two remaining cycles in Fig. 2 illustrate the evolution of σ above that temperature with the plateaus at 1138 and 1158 K both conducted for 12 h. A minor change in conductivity is observed at 1138 K while the conductivity degrades continuously at 1158 K. For

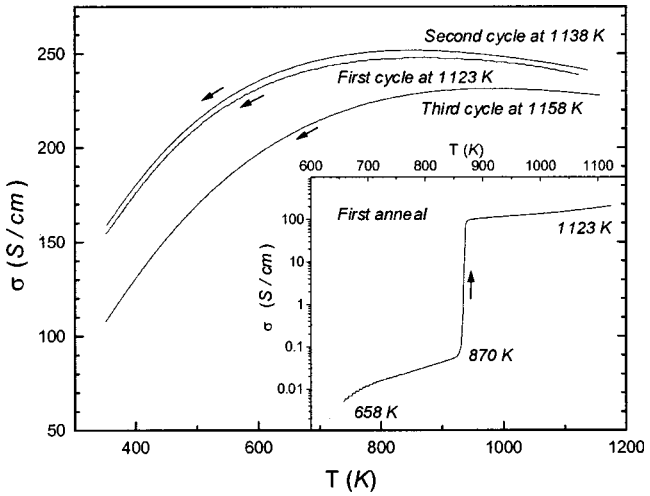

FIG. 2. Conductivity as a function of temperature during the annealing of an amorphous LSM5 thin film through three successive cycles at 1123, 1138, and 1158 K, respectively. For clarity reasons, only data recorded during cooling are shown. The insert shows the first annealing of the film.

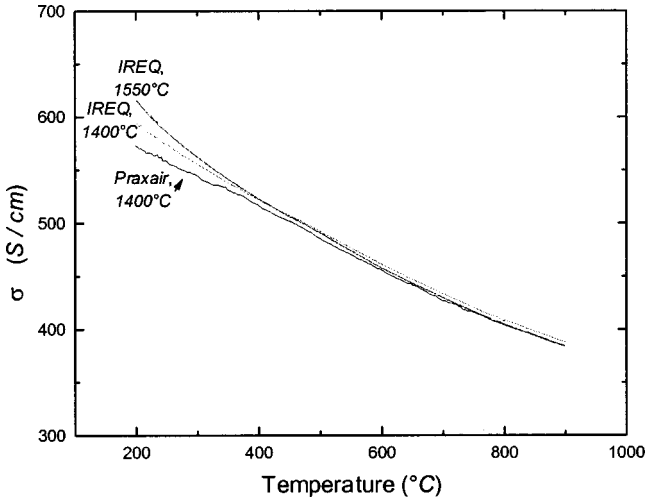

FIG. 4. High temperature conductivity variation for three different bulk LSM5 samples.

all remaining thin film samples a first anneal for one hour at 1123 K in air was used in order to maintain the best reproducibility within any one sample.

In Fig. 3, measurements from 12 to 300 K on a LSM5 thin film have been combined with those performed with the high temperature setup on the same sample. These data join smoothly and an interesting thermal behavior is thus observed. In the low temperature range, the conductivity decreases with T down to a minimum close to room temperature ($T \sim 285$ K). Beyond this temperature, it increases with increasing T. This behavior is predicted by the polaronic model[28] as we shall show later.

The high temperature conductivity behaves rather differently in bulk samples as shown in Fig. 4 where electrical data for three different samples are presented. The conductivity is significantly larger for bulk samples. Moreover, it decreases continuously as the temperature is raised. Data from the bulk samples either made from different starting powders or sintered at different temperatures are almost coincident. Sample "IREQ 1550 °C" was prepared as sample "IREQ 1400 °C," sintered at 1400 °C, except for a further anneal at 1550 °C which increased the average grain size from 1.8 to 4.5 μm. This increase produces a small increase in conductivity at the low end of the measured temperature range. Further experiments at 1173 K, with the oxygen partial pressure varied between 10^{-5} and 1 atm for several hours, showed no effect of this parameter upon the electric conductivity of bulk samples.

In Fig. 5, the available results on LSM5 from the literature are compared with the present measurements. Curves from the literature are either taken directly or the originally fitted curves converted to present coordinates. Reference 8 has been omitted due to the exceedingly low density of about 4.4 g/cm^3 reported for LSM5 samples in that study. All bulk samples in Fig. 5 tend to show a decrease in conductivity with increasing temperature. However, absolute conductivity values vary significantly from one set of data to another, the

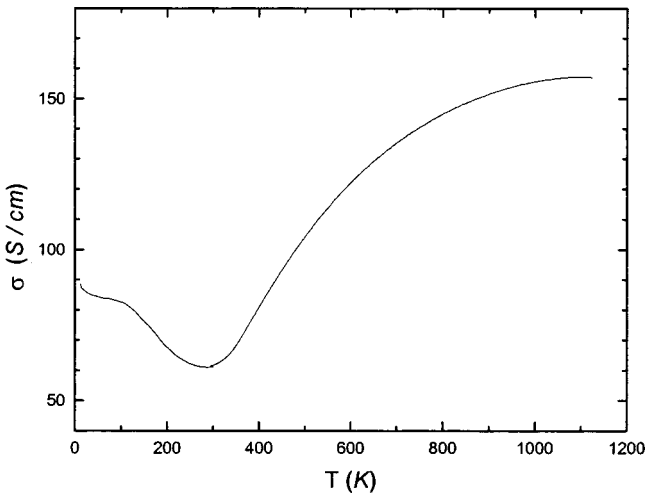

FIG. 3. Conductivity variation of a LSM5 thin film between 12 and 1123 K.

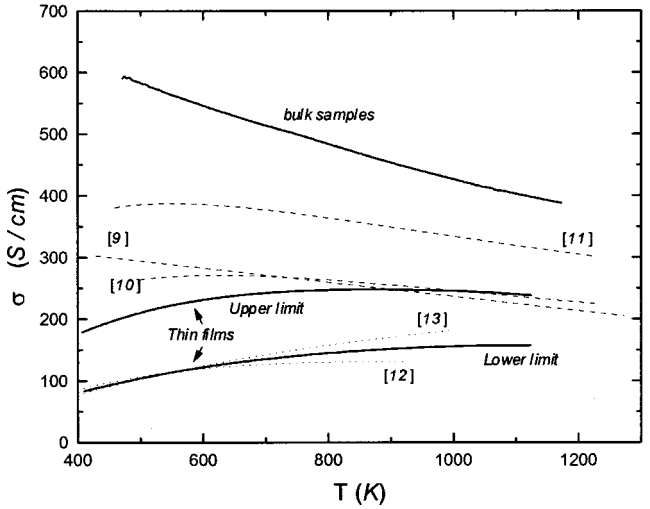

FIG. 5. Comparison of various conductivity data from bulk and thin film LSM5 samples. Solid, dashed, and dotted lines stand, respectively, for this study, bulk samples, and thin film samples from the literature. The number in brackets indicate the reference from which data were taken.

data from this study representing about twice the conductivity of the mean bulk values from the literature. Such a discrepancy cannot be totally explained with the available information from the literature. At this point, it can only be emphasized that the data from this study are highly reproducible and correspond to single-phase and almost fully dense samples from well-characterized powders. The picture is somewhat different for the thin film samples. Although, the conductivity values are highly reproducible within any sample, it may vary largely for different samples prepared at different times. The solid curves in Fig. 5 represent the upper and lower limits observed for samples from this study. The two data sets available from the literature correspond to sputtered films and agree well with our lower limit. The results for films appear to be quite different from those for bulk samples, showing increasing conductivity with temperature and systematically lower conductivities. It will now be shown that such a discrepancy is only apparent, readily explained by polaronic transport.

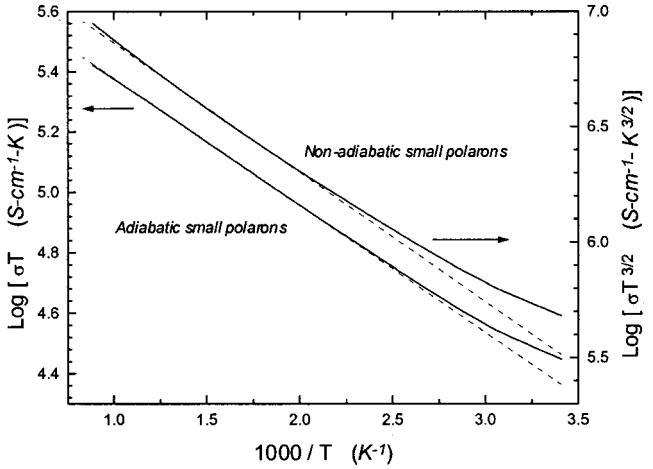

FIG. 6. Fits to high temperature conductivity measurements on a LSM5 thin film (upper limit) using both the adiabatic and nonadiabatic small polaron models.

IV. DISCUSSION

An important part of our knowledge on transport process is based on the analysis of mobility measurements within the framework of the proposed models and mechanisms. For carriers with mobility over 1 $cm^2/V\cdot s$, it is possible to discuss the electrical conductivity within the band formalism. However, for mobilities below 0.1 $cm^2/V\cdot s$, the band treatment is not appropriate. Therefore, it becomes necessary to use a generalized transport theory where the carrier-phonon interaction will not be treated as a perturbation but as the principal interaction from which the transport properties follow. With some assumptions as to the thermal behavior of the carrier density, $n(T)$, it will be shown that mobility in LSM5 can be extracted from conductivity measurements and that its value is too low for band conduction. This argument can be used to exclude metallic or semiconductor mechanisms as possible processes for conduction in LSM5.

If the particle-lattice interaction is strong enough, delocalized electrons or holes can be trapped within potential wells created by the displacement of atoms from their carrier-free equilibrium position. The quasiparticle formed by the carrier and the lattice distortion (phonons) is called a ''polaron.'' If the carrier is localized mainly in one unit cell, the small polaron model is applicable. Electronic transport by small polarons will lead to an activated behavior at high temperature and to nearly metallic band conduction at low temperature.

A. High temperature small polaron transport

At high temperature, conduction results from carriers which hop from one site to the other. In the adiabatic case (Emin–Holstein model),[22] the carrier adjusts rapidly to the motion of the lattice and, on coincidence between the energies of neighboring sites, is very likely to hop to the neighboring site. In this case σ_{hop} is given by

$$\sigma_{\text{hop}} = ne\mu = \frac{3}{2}\frac{ne^2a^2\nu_0}{k_B}\frac{1}{T}\exp\left(-\frac{W_P - 2J}{2k_BT}\right), \qquad (1)$$

where n is the polaron density, e the electronic charge, μ the polaron mobility, a the hopping distance, and k_B, the Boltzmann constant. In this equation, ν_0 is the frequency of optical phonons, assuming no dispersion.[24] This is the effective frequency at which the carrier tries to hop to a neighboring site. The factor of 3/2 takes account of the fact that the polarons move in a three-dimensional lattice.[22] The Boltzmann factor, with W_P standing for the polaron binding energy, expresses the probability that two neighboring sites be in coincidence. Since the carrier moves more rapidly than the lattice, it can hop back and forth many times between two sites before lattice relaxation occurs. The carrier's kinetic energy, which corresponds to half the electronic bandwidth for a rigid lattice, J, will then reduce the hopping energy, W_H [in Eq. (1), $W_H = W_P/2 - J$]. For this case, conductivity measurements fitted to a $\log(\sigma T)$ vs $1/T$ plot should lead to a straight line.

In the nonadiabatic case (Holstein model),[28] the carrier moves too slowly in comparison with the lattice distortion and relaxation, and thus, it misses many coincidence events before hopping. Conductivity is then given by

$$\sigma_{\text{hop}} = \frac{ne^2a^2}{k_B}\frac{\pi J^2}{h}\left(\frac{2\pi}{W_pk_B}\right)^{1/2}\frac{1}{T^{3/2}}\exp\left(-\frac{W_P}{2k_BT}\right), \qquad (2)$$

where h is Planck's constant.[28] As opposed to the adiabatic model, data should be fitted to a $\log(\sigma T^{3/2})$ vs $1/T$ plot to obtain straight lines. Thus, the activation energy obtained from the nonadiabatic model will be higher than the adiabatic value, and the data interpretation will be quite different.

Conductivity measurements for LSM5 have been interpreted in both the adiabatic and the nonadiabatic polaronic models. Figure 6 shows thin film data (upper limit) fitted to each model. Equations for the corresponding linear relationships are further presented in Table II along with the corresponding linear correlation coefficients, R^2. Although both models fit the data reasonably well, the better correlation coefficient obtained with the adiabatic model for all three cases is an indication in favor of the adiabatic behavior in LSM5.

TABLE II. Equation and linear correlation coefficient of the straight lines fitted to the experimental data for thin films and bulk using both the adiabatic and nonadiabatic models.

	Adiabatic		Non-adiabatic	
	Equation	R^2	Equation	R^2
Bulk	$\log(\sigma T) = -173.2/T + 5.8044$	0.9996	$\log(\sigma T^{3/2}) = -349.8/T + 7.7811$	0.9978
Thin film (upper limit)	$\log(\sigma T) = -365.2/T + 5.7532$	0.9999	$\log(\sigma T^{3/2}) = -510.1/T + 7.3915$	0.9984
Thin film (lower limit)	$\log(\sigma T) = -477.1/T + 5.6646$	0.9991	$\log(\sigma T^{3/2}) = -629.9/T + 7.3127$	0.9976

By combining the fitting equations in Table II with the conductivity equations for both adiabatic and nonadiabatic behavior [Eqs. (1) and (2)], some of the physical parameters for conductivity in LSM5 bulk and thin film samples can be extracted, and are given in Table III. In lanthanum manganite, ν_0 is associated with the principal vibration mode of the Mn–O bonds near 554 cm^{-1} (1.66×10^{13} Hz)[14] and the hopping distance, a, is the distance between two neighboring Mn sites, e.g., 0.39 nm.[29] Based on the assumption of adiabatic behavior, the polaron densities are evaluated. For bulk samples, $n=(9.1\pm0.5)10^{21}\,cm^{-3}$ and for thin films, n ranges from $(7\pm1)10^{21}$ to $(8\pm1)10^{21}\,cm^{-3}$. It is interesting to note that the polaron density is almost the same in bulk samples and thin films, even if their conductivity thermal behavior is quite divergent. This was to be expected, since the polaron density results from stoichiometric doping (i.e., it should present only a weak dependence on temperature). In fact, the expected polaron density can be easily evaluated. For each two unit cells in LSM5, La^{+3} is replaced by Sr^{+2} releasing an electron. Given that the unit cell volume is $(0.39\ nm)^3$, the nominal polaron density should be around $8.4\times10^{21}\,cm^{-3}$. This theoretical estimate is in good agreement with values deduced from the experimental results.

The hopping energy is calculated both for the adiabatic and the nonadiabatic models from the slope of the fitted curves for conductivity. In the adiabatic case, $W_H=34$ meV for bulk samples and ranges from 73 to 99 meV for thin films. The nonadiabatic case leads to higher values. Although polaron density remains almost the same for all LSM5 samples, such is not the case regarding W_H. This parameter may vary not only between bulk conductivity data from different sources, but also between films annealed under different conditions. Correlated hopping might explain the relatively small W_H observed in bulk samples.[20] But this effect cannot explain the difference in W_H between thin film samples prepared in almost the same conditions. In a previous article,[7] it has been shown that polycrystalline films annealed within the same conditions present small morphological variations (e.g., the grain sizes). According to some reported observations,[30–32] W_H might be a function of the crystal unit cell deformation and, more precisely, of the angle between the Mn–O–Mn bonds, the relaxed structure leading to a minimum in W_H. Thus, any difference in grain sizes, leading to different mean cell deformation, should result in different hopping energy.

TABLE III. Physical parameters obtained from conductivity thermal behavior analysis. Some of the bulk and thin film results are expressed in both the adiabatic and nonadiabatic models.

		Bulk	Thin film (upper limit)	Thin film (lower limit)
n (cm^{-3})	Adiabatic	9.1×10^{21}	8×10^{21}	7×10^{21}
W_H (meV)	Adiabatic	34	73	99
	Nonadiabatic	70	100	126
W_p (meV)	Nonadiabatic	140	200	254
J (meV)	Nonadiabatic	47	49	51
J_{max} (meV)	300 K	28	30	32
	1000 K	38	40	43

The Holstein nonadiabatic model is based on the assumption that J (which is also the electronic orbital overlap integral) can be treated as a perturbation in the corresponding Schrödinger equation. Thus, this approach is only valid for low values of J. In the high temperature region there is a condition on J for which the non-adiabatic treatment is valid. This condition is given by

$$J \ll J_{\max} = W_P^{1/4}\left(\frac{k_B T}{\pi}\right)^{1/4}\left(\frac{h\nu_0}{\pi}\right)^{1/2}. \tag{3}$$

When J becomes higher than J_{max}, the nonadiabatic model is no longer valid and we should discuss the data in the adiabatic model.[28]

Taking the nonadiabatic fit for the bulk samples (Table II), 140 meV is found for the polaron binding energy, W_P. Now with W_P, a, n, and Eq. (2) on hand, a value of 47 meV is calculated for the nonadiabatic J. Values obtained for the thin film lower and upper limit are almost the same as the one calculated for bulk. This result was expected because the electronic orbital overlap integral mostly depends on the sample composition.

Equation (3) is then used for the estimation of J_{max} at various temperatures, leading to $J_{max}(300\,K)=27$ meV and $J_{max}(1000\,K)=37$ meV. Since that J_{max} is lower than the nonadiabatic value over the temperature range studied, the nonadiabatic model is not valid as a description of the thermal behavior of the conductivity. Similar conclusions in favor of the adiabatic small polaron mechanism model are also reached for thin films. In what follows, results will be treated according to the adiabatic model.

B. Low temperature small polaron transport

One of the most interesting conclusions of the polaronic model is that at very low temperature the zero point energy allows the polaron to hop to a neighboring site without thermal activation, dragging the lattice polarization.[28] At tem-

peratures lower than $\theta_D/2$ (where, θ_D, is the Debye temperature of the material), the polaron can then be seen as a heavy charge carrier with a behavior described by the usual band formalism.[33] In this temperature range, the material can be treated as a doped polaronic semiconductor.[34]

In this section, we will show that polaronic transport is the prevalent mechanism over the whole temperature range. In the polaronic model, it is well accepted that transport is dominated by a hopping process at high temperature and by tunneling at low temperature. In the previous section, it has been shown that far from $\theta_D/2$, in the high temperature region, conductivity is well described by Eq. (1). In the very low temperature region, conductivity can be described by two different mechanisms in series

$$\sigma_{\text{low}}=\frac{\sigma_0\sigma_{\text{tun}}}{\sigma_0+\sigma_{\text{nm}}}, \tag{4}$$

where σ_0 is a constant conductivity, included using Matheissen's rule, which takes into account the different scattering processes that becomes important in this temperature range.[35] In this equation, σ_{tun} is given by[34]

$$\sigma_{\text{tun}}=\frac{ne^2a^2J^2}{h^2k_B}\left(\frac{W_H}{J}\right)^4\left(\frac{\Delta\nu}{\nu_S^2}\right)\exp(-2\gamma^2)\frac{1}{T}\sinh^2\left(\frac{h\nu_S}{2k_BT}\right), \tag{5}$$

where $\Delta\nu$ is the phonon dispersion and ν_S is the frequency of the softest optical phonon branch (related to the tilting of the oxygen octahedra).[35] The interaction constant γ describes the interaction between the lattice and the charge carrier. It represents the ratio of the polaron binding energy to the kinetic energy of the lattice at a certain wave number (the number of phonons surrounding the charge carrier). This also describes the polaronic band narrowing. In the very low temperature region (i.e., when $T<\theta_D/4$), the zero point movement is dominant; hence, the interaction constant does not change significantly with T and equals γ_0. For higher temperature, this quantity will depends on T as

$$\gamma=\gamma_0\left(1+\frac{4k_BT}{h\nu_0}\right) \quad \text{for} \quad T>\theta_D/4\,. \tag{6}$$

This will lead to an exponential decrease of the conductivity with T. Equation (6) is valid for the nonadiabatic case. For the adiabatic case, the same thermal behavior is expected, but the decrease will be slightly slower.[33]

The insert in Fig. 7 shows the very low temperature conductivity measurements (extracted from Fig. 3) and fitted with Eq. (5) and $\gamma=\gamma_0$. The values below 50 K are not taken into account in this fit, their divergence from the model may results from another mechanism. From the fit, σ_0 and ν_S can be extracted directly, leading to 84.3 S/cm and 2.5×10^{12} Hz, respectively. This value of ν_S is in good agreement with values published in Ref. 35. Under the assumption that J can be estimated by $J_{\max}(75\,\text{K})=22$ meV over this temperature range and that the polaron density is constant, we obtain

$$\Delta\nu\exp(-2\gamma_0^2)=6\times10^{10}\ \text{Hz}. \tag{7}$$

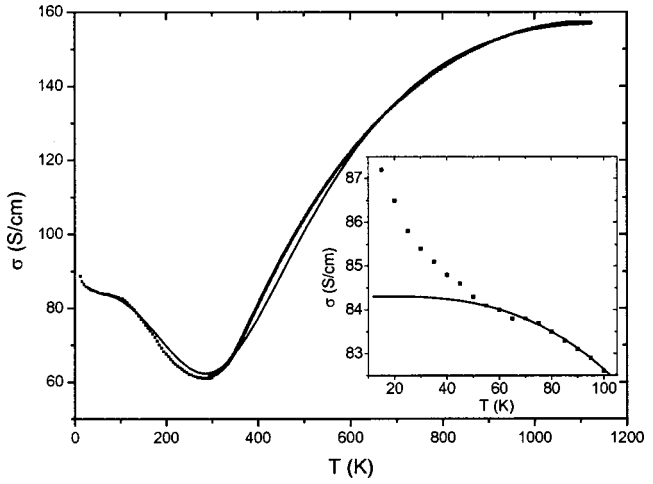

FIG. 7. Conductivity measurements for a LSM5 thin film (lower limit) fitted with Eq. (8) from 50 to 1123 K. The filled squares are experimental data and the continuous line is Eq. (8) with parameters of Table IV. The insert shows the very low temperature conductivity measurements fitted with Eq. (5) and with $\gamma=\gamma_0$.

In order to obtain total conductivity over the whole temperature range, the low temperature and hopping contributions must be added in parallel. Total conductivity is given by

$$\sigma_{\text{tot}}=\sigma_{\text{low}}+\sigma_{\text{hop}}\,. \tag{8}$$

It is now possible to fit the results from $\theta_D/4(\approx130\,\text{K})$ to 1123 K in order to obtain the best value for γ_0, which is 0.35. With this value and Eq. (7), the phonon dispersion can be extracted: $\Delta\nu=8\times10^{10}$ Hz.

Figure 7 shows the experimental results of Fig. 3 fitted between 50 and 1123 K with Eq. (8) (parameters used are listed in Table IV). As one can see, this simple polaronic model explains the experimental measurements quite well over the whole temperature range. Moreover, all parameters used to fit the data are physically reasonable.

Recently, in their model for colossal magnetoresistance in doped manganites, Alexandrov and Bratkovsky have proposed that the minimum in total conductivity observed at the critical temperature of transition (T_C), might be the result of what they called a current-carrier-density collapse (CCDC). They proposed that over the critical temperature, in the paramagnetic state, an important fraction of the carriers is bound into immobile bipolarons instead of being mobile polarons. As the temperature decreases in the paramagnetic phase ($T>T_C$), so does the density of mobile polarons, and the conductivity quickly decreases with the decline of the number of

TABLE IV. Values used to fit conductivity measurements over the whole temperature range [Thin film (lower limit)].

Parameters	Values	Parameters	Values
a (m)	0.39×10^{-9}	n (cm^{-3})	7×10^{21}
W_H (meV)	99	ν_0 (Hz)	1.66×10^{13}
J (meV)	22	ν_s (Hz)	2.5×10^{12}
γ_0	0.35	$\Delta\nu$ (Hz)	8×10^{10}
σ_0 (S/cm)	84.3		

carriers. With the onset of ferromagnetic order at T_C, the pairs break up, the density of carriers jumps up, and the conductivity suddenly increases, as observed experimentally. Since a simple polaronic model using a constant polaron density is able to describe experimental data over the whole temperature range, it seems that the CCDC predicted by Alexandrov and Bratkovsky is weak or simply not observed in LSM5 when no magnetic field is applied.

V. CONCLUSION

Conductivity measurements showed that the single-phase and almost fully dense LSM5 bulk samples yield relatively reproducible results. For thin film samples, conductivity values are highly reproducible for any sample, but may vary widely between samples prepared at different times. Even if the conductivity is lower than in bulk, these data are still higher than previously reported in the literature for thin films. The study of conductivity over a wide range of temperature has shown that electronic transport in LSM5 is well described by the Emin–Holstein adiabatic small polaron model. Even if the thermal behavior of the conductivity seems to be quite different in bulk and thin film samples, the polaronic model describes all data quite well. Physical parameters have been extracted from conductivity measurement with this model. It has been shown that for both types of samples, the carrier density is nearly the same as the nominal LSM5 carrier density ($n_{\mathrm{LSM5}}=8.4\times10^{21}\,\mathrm{pol/cm^3}$). For thin films, the hopping energies W_H lie between 73 and 99 meV and remain almost constant at 34 meV for bulk samples. Using a simple polaronic model with a constant polaron density, conductivity measurements on a thin film have been fitted quite well from 50 to 1123 K. From this model, different physical parameters have been extracted: $\nu_S=2.5\times10^{12}\,\mathrm{Hz}$, $\Delta\nu(\mathrm{Hz})=8\times10^{10}\,\mathrm{Hz}$, and $\gamma_0=0.35$. We find no evidence of CCDC for the LSM5 thin film.

ACKNOWLEDGMENTS

The authors thank the Natural Sciences and Engineering Research Council of Canada (NSERC) and Hydro-Quebec Research Institute (IREQ) for financial support. They also acknowledge Philippe Decorse, Suzie Poulin, and Abdeltif Essalik for useful discussions and Jean-Paul Lévesque for technical support.

[1] C. N. R. Rao, R. Mahesh, A. K. Raychaudhuri, and R. Mahendiran, J. Phys. Chem. Solids **59**, 487 (1998).
[2] A. Urushibara, Y. Moritomo, T. Arima, A. Asamitsu, G. Kido, and Y. Tokura, Phys. Rev. B **51**, 14103 (1995).
[3] N. Zhang, W. Ding, W. Zhong, D. Xing, and Y. Du, J. Mater. Sci. **34**, 1829 (1999).
[4] W. Feduska and A. O. Isenberg, J. Power Sources **10**, 89 (1983).
[5] A. Hammouche, E. Siebert, and A. Hammou, Mater. Res. Bull. **24**, 367 (1989).
[6] E. Quenneville, P. Decorse, M. Meunier, F. Morin, and A. Yelon, in *Proceedings of the Symposium on Solid State Ionic Devices*, edited by E. D. Wachsman, J. Akridge, M. Liu, and N. Yamazoe (The Electrochemical Society, Pennington, NJ, 1999), Proc. 99-13, p. 218.
[7] P. Decorse, E. Quenneville, S. Poulin, M. Meunier, F. Morin, and A. Yelon, J. Vac. Sci. Technol. A **19**, 910 (2001).
[8] K. Katayama, T. Ishihara, H. Ohta, S. Takenchi, Y. Esaki, and E. Inukai, Nippon Seramikkusu Kyokai Gakujutsu Ronbunshi **97**, 1327 (1989).
[9] H. Lauret, E. Caignol and A. Hammou in *Proceedings of the 2nd International Symposium on Solid Oxide Fuel Cells*, edited by F. Gross, P. Zegers, S. C. Singhal, and O. Yamamoto, Commission of European Communities, Rep. No EUR 13546 EN, 1991, p. 479.
[10] J. A. M. van Roosmalen, J. P. P. Huijsmans, and L. Plomb, Solid State Ionics **66**, 279 (1993).
[11] A. Mackor, T. P. M. Koster, J. G. Kraaijkamp, J. Gerretsen, and J. P. G. M. van Eijk, in *Proceedings of the 2nd International Symposium on Solid Oxide Fuel Cells*, edited by F. Gross, P. Zegers, S. C. Singhal, and O. Yamamoto, Commission of European Communities, Rep. No EUR 13546 EN, 1991, p. 463.
[12] B. Gharbage, F. Mandier, H. Lauret, C. Roux, and T. Pagnier, Solid State Ionics **82**, 85 (1995).
[13] Y. Takeda, R. Kanno, M. Noda, Y. Tomida, and O. Yamamoto, J. Electrochem. Soc. **134**, 2656 (1987).
[14] A. Machida, Y. Moritomo, and A. Nakamura, Phys. Rev. B **58**, 8, R4281 (1998).
[15] S. Yoon, H. L. Liu, G. Schollerer, S. L. Cooper, P. D. Han, D. A. Payne, S.-W. Cheong, and Z. Fisk, Phys. Rev. B **58**, 2795 (1998).
[16] Y. G. Zhao *et al.*, Phys. Rev. Lett. **81**, 1310 (1998).
[17] M. Jaime, M. B. Salomon, M. Rubinstein, R. E. Treece, J. S. Horwitz, and D. B. Chrisey, Phys. Rev. B **54**, 11914 (1996).
[18] M. F. Hundler and J. J. Neumeier, Phys. Rev. B **55**, 11511 (1997).
[19] E. O. Ahlgren and F. W. Poulsen, Solid State Ionics **86–88**, 1173 (1996).
[20] D. Emin, Phys. Rev. Lett. **25**, 1751 (1970).
[21] M. Jaime, H. T. Hardner, M. B. Salomon, M. Rubinstein, P. Dorsey, and D. Emin, Phys. Rev. Lett. **78**, 951 (1997).
[22] D. Emin and T. Holstein, Ann. Phys. **53**, 439 (1960).
[23] J.-S. Zhou and J. B. Goodenough, Phys. Rev. B **58**, R579 (1998).
[24] W. E. Spear, J. Non-Cryst. Solids **1**, 197 (1969).
[25] R. Izquierdo, F. Hanus, Th. Lang, D. Ivanov, M. Meunier, L. Laude, J. F. Currie, and A. Yelon, Appl. Surf. Sci. **96–98**, 855 (1996).
[26] F. Morin, in Proceedings of the 3rd European Solid Oxide Fuel Cell Forum, edited by P. Stevens, 1998, p. 193.
[27] H. Tagawa, N. Mori, H. Takai, Y. Yonemura, H. Minamiue, H. Inaba, J. Mizusaki, and T. Hashimoto, in *Proceedings of the 5th International Symposium on Solid Oxide Fuel Cells*, edited by U. Stimming, S. C. Singhal, H. Tagawa, and W. Lehnert (The Electrochemical Society, Pennington, NJ, 1997), Proc. 97-40, p. 785.
[28] T. Holstein, Ann. Phys. **8**, 343 (1959).
[29] J. M. D. Coey, M. Viret, and L. Ranno, Phys. Rev. Lett. **75**, 3910 (1995).
[30] J. Fontcuberta, B. Martínez, A. Seffar, S. Pinol, J. L. García-Munoz, and X. Obradors, Phys. Rev. Lett. **76**, 1122 (1996).
[31] D. C. Worledge, G. J. Snyder, M. R. Beasley, T. H. Geballe, R. Hiskes, and S. DiCarolis, J. Appl. Phys. **80**, 5158 (1996).
[32] J. M. De Teresa, K. Dörr, K. H. Müller, and L. Schultz, Phys. Rev. B **58**, R5928 (1998).
[33] I. G. Austin and N. F. Mott, Adv. Phys. **18**, 41 (1969).
[34] A. S. Alexandrov and A. M. Bratkovsky, J. Phys.: Condens. Matter **11**, 1989 (1999).
[35] G.-M. Zhao, V. Smolyaninova, W. Prellier, and H. Keller, Phys. Rev. Lett. **84**, 6086 (2000).